

Direct Numerical Solution of the Steady 1D Compressible Euler Equations for Transonic Flow Profiles with Shocks

Hans De Sterck and Scott Rostrup

Department of Applied Mathematics, University of Waterloo, Ontario, Canada

Email: *hdesterck@uwaterloo.ca, sarostru@uwaterloo.ca*

ABSTRACT

It is well-known that stationary transonic solutions of the compressible Euler equations are hard to compute using the stationary form of the equations. Therefore, time marching methods with explicit or implicit time integration are normally employed. In this paper a method is described that computes one-dimensional transonic flows directly from the stationary equations. The method is based on a dynamical systems formulation of the problem and uses adaptive integration combined with a 2×2 Newton method. Example calculations show that the resulting method is fast and accurate. A sample application area for this method is the calculation of transonic hydrodynamic escape flows from extrasolar planets and the early Earth, and the method is also illustrated for quasi-one-dimensional flow in a converging-diverging nozzle. The method can be extended easily to handle flows with shocks, using a Newton method applied to the Rankine-Hugoniot relations in order to match the shock location with the outflow boundary condition.

1 INTRODUCTION

In this paper we introduce a direct numerical approximation algorithm for steady one-dimensional (1D) transonic flow solutions of the Euler equations of gas dynamics. In the first part of the paper, we consider outflow solutions of the radial compressible Euler equations with gravity and heat source terms:

$$\frac{\partial}{\partial t} \begin{bmatrix} \rho r^2 \\ \rho u r^2 \\ \left(\frac{\gamma p}{\gamma-1} + \frac{\rho u^2}{2}\right) r^2 \end{bmatrix} + \frac{\partial}{\partial r} \begin{bmatrix} \rho u r^2 \\ \rho u^2 r^2 + p r^2 \\ \left(\frac{\gamma p}{\gamma-1} + \frac{\rho u^2}{2}\right) u r^2 \end{bmatrix} = \begin{bmatrix} 0 \\ -\rho GM + 2pr \\ -\rho GMu + q_{heat} r^2 \end{bmatrix}. \quad (1)$$

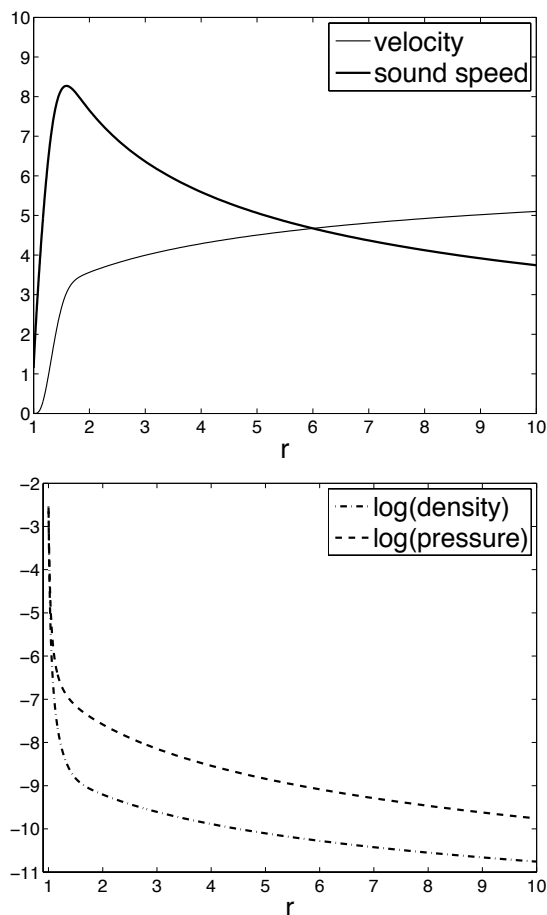


Figure 1: Radial transonic flow solution for $GM \approx 2.6 \times 10^2$, and $q_{heat} = A_0 \exp(-10(r - 1.1)^2)$ with $A_0 \approx 4.4 \times 10^{-6}$. Density and pressure values at the inflow boundary $r_a = 1$ are $\rho \approx 2.9 \times 10^{-3}$ and $p \approx 2.7 \times 10^{-3}$. Note the decimal logarithm scale on the density and pressure plot.

Here, ρ is the fluid mass density, p is the pressure, u is the radial velocity, r is the radial coordinate, t is time, $-\rho GM/r^2$ is the gravitational force density, and γ is the adiabatic constant. With G being the universal gravity constant and M the mass of the outflow object, we take $GM = 15$ in normalized units for all the test problems in this paper. Throughout this paper the value $\gamma = 7/5$ for di-atomic gases is used. The right hand side of the equation contains a heat source term q_{heat} . The sound speed c , the temperature T , the entropy S , and the Mach number M of the perfect gas are defined by $c^2 = \gamma p/\rho$, $T = p/\rho = c^2/\gamma$, $S = p/\rho^\gamma$, and $M = u/c$ in our choice of units.

As illustrated in Fig. 1, these equations allow for stationary transonic outflow solutions, where the radial flow velocity is initially subsonic, but then passes through a critical point where $u = c$, and subsequently takes on supersonic values beyond the critical point. This type of flow has applications in models of hydrodynamic escape from extrasolar planets and the early Earth [1, 2]. Fig. 1 shows a transonic solution of Eq. (1) for parameters that are representative for the extrasolar planet case [1]. In our planetary atmosphere calculations, one of the major quantities of interest to be obtained by numerical simulation is the radial outflow flux $F = \rho ur^2$, and we want to determine how this radial mass flux varies as a function of the heating profile and the density and pressure imposed at the inflow boundary.

Most traditional methods for computing stationary transonic solutions start from the time-dependent form of the equations, rather than its stationary counterpart. Some initial condition is advanced in time until a stationary solution is reached. Standard explicit finite volume methods [3] for Eq. (1) may require many thousands of timesteps to converge, also depending on the grid size and the resulting CFL condition. Several methods have been introduced that accelerate convergence, including local timestepping and implicit timestepping. In particular, important advances for solving stationary Euler problems have been made through the technique of local preconditioning (see [4, 5], and references therein).

In addition to slow convergence, a second major concern with existing methods for stationary Euler flow calculations is that the resulting flow profiles may not be sufficiently accurate [4]. The planetary outflow solutions targeted in our work are especially challenging in terms of accuracy. For example, Fig. 1 shows that, over a very small range close to the inner boundary, density and pressure may drop by six and four orders of magnitude, respectively. The method we propose in this paper allows, in a straightforward way, to employ adaptive refinement in this region that is based on rig-

orous error estimation.

Driven by this generally unsatisfactory state of affairs in terms of convergence speed and flow profile accuracy, we have developed an approach for calculating radial transonic flow profiles that is based on directly solving the stationary problem, rather than using time-relaxation of the hyperbolic system (1). An important reason why the stationary route is normally not considered, is related to difficulties with the number of boundary conditions. For example, the problem in Fig. 1 has only two boundary conditions (at the inflow boundary), and it is not clear how that allows for solving the three equations in three unknowns of the stationary problem. In contrast, if this problem is solved by hyperbolic time-relaxation using Eq. (1), the boundary conditions can be handled in a standard way: a subsonic inner boundary with two inflow conditions and one outflow condition, and a supersonic outer boundary with three outflow conditions. However, aided by insight derived from a dynamical system representation of the stationary equations, it is possible to find a solution for the boundary condition problem for the stationary equation, as is explained below.

This paper is organized as follows. In Section 2, we explain the first important component of our algorithm, using a simple isothermal Euler example problem. The second component of the algorithm is explained in Section 3. The algorithm is illustrated there for the case of radial outflow solutions of the Euler equations with gravity and heat source terms. Section 4 describes how the method can be extended to handle transonic flows with shocks. This is illustrated for nozzle flow with a shock. Finally, conclusions are formulated in Section 5.

2 A CRITICAL POINT METHOD FOR ISOTHERMAL EULER FLOWS

In this section, we illustrate the first essential component of our algorithm for calculating transonic flow profiles of the Euler equations. This ingredient of the algorithm is best illustrated for the simplified case of the isothermal Euler equations. A decoupled equation for $u(r)$ can be isolated from the stationary form of the radial isothermal Euler equations, resulting in

$$\frac{du}{dr} = \frac{2uc^2 \left(r - \frac{GM}{2c^2} \right)}{r^2 (u^2 - c^2)}. \quad (2)$$

The sound speed c is now a constant to be specified. This equation can be integrated easily. Fig. 2 shows solutions for various values of the integration constant, for the case $GM = 2$ and $c = 1$. Note that there is only

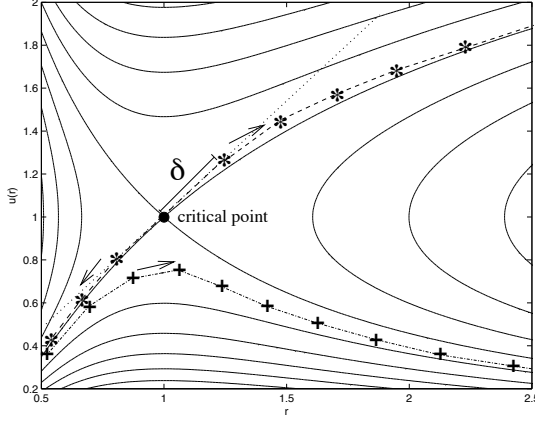


Figure 2: Solution curves $u(r)$ for the isothermal Euler equations with $GM = 2$ and $c = 1$. Numerical integration from the left boundary (dash-dotted curve) does not allow to approximate the transonic solution, but integration in two directions outward from the critical point (dashed curves) leads to an accurate numerical approximation of the transonic curve. The arrows indicate the direction of numerical integration. The two starting points for the numerical integration are chosen a distance δ away from the critical point.

one transonic outflow solution: the transonic conditions $u(r_a) < c$ and $u(r_b) > c$ fully specify the unique transonic outflow solution of Eq. (2), and no further boundary information is required. In contrast, specifying any of the other solution curves requires a boundary condition.

Eq. (2) can be written as a dynamical system as follows:

$$\begin{aligned} \frac{du(s)}{ds} &= -2u(s)c^2 \left(r(s) - \frac{GM}{2c^2} \right), \\ \frac{dr(s)}{ds} &= -r(s)^2 (u(s)^2 - c^2), \end{aligned} \quad (3)$$

or, in matrix form,

$$\frac{d\mathbf{V}}{ds} = \mathbf{G}(\mathbf{V}), \quad (4)$$

with the state vector given by $\mathbf{V} = [u(s) \ r(s)]^T$. The solutions $u(s)$, $r(s)$ of this dynamical system – which are also called solution trajectories – are parametrizations of the solution curves of Fig. 2. The critical point (or equilibrium point) of this dynamical system is attained when the right hand side of Eq. (4) vanishes,

which leads to the conditions

$$\begin{aligned} r_{crit} &= \frac{GM}{2c^2}, \\ u_{crit} &= c. \end{aligned} \quad (5)$$

For our choice of the parameters GM and c , the critical point is the point $(1, 1)$ in the (r, u) phase plane of Fig. 2. Note that du/dr in Eq. (2) is undefined at the critical point. The equilibrium point is of saddle-point type, since the eigenvalues of the Jacobian matrix of $\mathbf{G}(\mathbf{V})$ evaluated at the equilibrium point have opposite signs.

Fig. 2 also provides some intuition as to what kind of numerical approach would be appropriate for approximating the transonic curve numerically, if an analytical solution were not known. The dash-dotted curve shows that numerical integration of Eq. (2) from the left boundary would not be successful, even if the velocity on the transonic solution curve at the left boundary were known, because rounding and truncation errors would make the numerical approximation deviate from the transonic branch, regardless how close the initial condition is chosen to the transonic solution. On the other hand, the dashed curves suggest that integration outward from the critical point may be a more viable idea. Using a local linearization of Eq. (4) about the critical point, the direction tangent to the transonic curve can be obtained. With initial points chosen at distance δ from the critical point in the direction tangent to the transonic curve, Eq. (2) can be integrated numerically in two directions away from the critical point. The trajectories are attracted toward the transonic curve as the integration progresses, resulting in an accurate numerical approximation of the transonic solution. The accuracy of the approximation can be increased by reducing δ and the integration step size. This method for calculating critical curves of dynamical systems is actually well-known and used often in the numerical study of dynamical system [6]. We have used an adaptive fourth-fifth order accurate Runge-Kutta ordinary differential equation (ODE) integrator for the results shown below (see, e.g., [7].) The reason why this method, which originates in dynamical systems research, works without change for this problem, is that the critical point for the isothermal Euler equations is known in advance, since all quantities in the right hand side of Eq. (5) are known constants. For the full Euler equations, however, the location of the critical point is not known *a priori*. In the next section the second important component of our algorithm is described, which allows the use of the above described integration technique even when the location of the critical point in the desired transonic solution is not known ahead of time.

3 A NEWTON CRITICAL POINT (NCP) METHOD FOR SMOOTH EULER FLOWS

We proceed as in the previous section by writing the spherically symmetric Euler equations (1) as a dynamical system:

$$\begin{aligned} \frac{dF}{ds} &= 0, \\ \frac{du}{ds} &= 2uc^2 \left(r - \frac{GM}{2c^2} \right) - (\gamma - 1) q_{heat} \frac{r^4 u}{F}, \\ \frac{dr}{ds} &= r^2 (u^2 - c^2), \\ \frac{dT}{ds} &= (\gamma - 1) T (GM - 2u^2 r) - (\gamma - 1) q_{heat} \frac{r^4}{F} (T - u^2). \end{aligned} \quad (6)$$

Note that the radial mass flux F is a constant of motion in the dynamical system. Some straightforward algebra shows that the critical point of this system is not uniquely defined. In fact, there is a two-parameter family of critical points, which can be parametrized, for instance, by the flux F_{crit} and the radius r_{crit} at the critical point. Using this parametrization, the critical temperature and velocity are given by

$$T_{crit} = \frac{GM}{2\gamma r_{crit}} + (\gamma - 1) \frac{q_{heat} r_{crit}^3}{2\gamma F_{crit}}, \quad (7)$$

$$u_{crit} = \sqrt{\gamma T_{crit}}. \quad (8)$$

Given a certain critical point defined by $\mathbf{C} = [F_{crit} \ r_{crit}]^T$, denote the density and pressure vector of the associated critical flow solution at the inflow boundary r_a by $\mathbf{B} = [\rho(r_a) \ p(r_a)]^T$. We can say that the critical point vector \mathbf{C} is mapped onto the inflow boundary vector \mathbf{B} by some mapping \mathbf{F} :

$$\mathbf{B} = \mathbf{F}(\mathbf{C}). \quad (9)$$

This mapping is provided by the transonic solution of Eq. (1) that passes through the critical point \mathbf{C} , and is a nonlinear mapping. Denote the target density and pressure at the inflow boundary by $\mathbf{B}^* = [\rho^*(r_a) \ p^*(r_a)]^T$. The critical point conditions \mathbf{C}^* that match the inflow boundary conditions \mathbf{B}^* can be determined efficiently by a Newton method that solves

$$\mathbf{B}^* = \mathbf{F}(\mathbf{C}). \quad (10)$$

In each Newton step, the current guess for the critical point parameter vector, $\mathbf{C}^{(k)}$, is improved by solving a

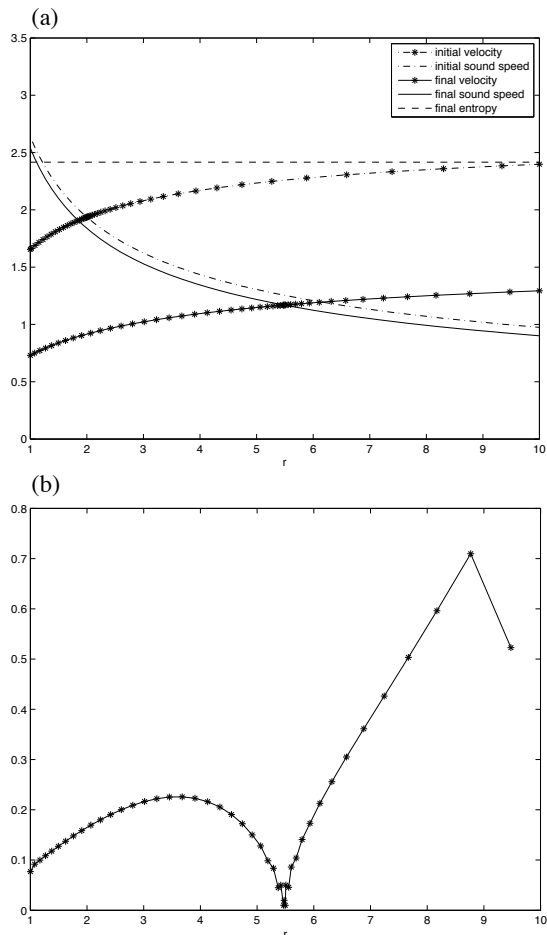


Figure 3: Radial transonic flow solution for $GM = 15$ and $q_{heat} = 0$, and with boundary conditions $\rho = 5$ and $p = 23$ at the inflow boundary $r_a = 1$. (a) Initial and final critical points and trajectories using the NCP algorithm. The algorithm proceeds by varying the critical point on the two-parameter manifold of critical points by use of a Newton method until the solution matches the specified boundary values. (b) Grid size values used by the adaptive integrator for the final solution obtained by the NCP algorithm. Smaller step sizes are selected close to the critical point, and near the inflow boundary where steep gradients are encountered.

linear system:

$$\mathbf{B}^* = \mathbf{F}(\mathbf{C}^{(k)}) + \left. \frac{\partial \mathbf{F}}{\partial \mathbf{C}} \right|_{\mathbf{C}^{(k)}} (\mathbf{C}^{(k+1)} - \mathbf{C}^{(k)}). \quad (11)$$

Here, the 2×2 Jacobian of function $\mathbf{F}(\mathbf{C})$ is determined by numerical calculation, which requires adaptive integration of three flow profiles, from the neighborhood of the current critical point guess to the inflow boundary.

Table 1: Newton method convergence for the NCP method applied to the problem of Fig. 3.

Newton step k	error $\ \mathbf{B}^{(k)} - \mathbf{B}^*\ _2$
1	4.41106268600662
2	2.28831581534917
3	1.43924405447424
4	0.10259052732943
5	0.00125578478131
6	0.00000037420499

Fig. 3(a) shows how the resulting algorithm is applied for the calculation of a transonic flow, starting from initial guess $\mathbf{C}^{(0)} = [F_{crit} \ r_{crit}]^T = [1 \ 2]^T$. Table 1 illustrates the convergence behaviour of the method. Convergence of the method is fast: only six Newton steps were needed to obtain convergence for the result of Fig. 3. This is significant: only 18 explicit integration sweeps over half of the computational domain downward from the critical point are needed as the Newton process proceeds, together with six inversions of a 2×2 linear system, and a final full integration sweep for the final solution. This is to be compared with the work required for time-relaxation methods. Explicit relaxation methods require up to several thousands of full integration sweeps. Relaxation methods based on implicit discretization of time-dependent Eq. (1) may also require only a limited number of Newton-like iterations, but each step requires the inversion of a large Jacobian matrix that contains all the discrete degree of freedoms, while in our approach the Newton system to be solved is a small 2×2 system. It is thus clear that the NCP method offers an efficient alternative to these existing methods. Fig. 4 shows an example of a flow profile calculated using the NCP method for a problem with a heat source term.

4 EXTENSION TO EULER FLOWS WITH SHOCKS

In this Section we repeat the analysis presented above for the case of a quasi-1D converging-diverging nozzle [8], leading to similar results. Fig. 5 shows a de Laval nozzle, in which subsonic flow can be accelerated to supersonic flow in a continuous fashion. If the cross-sectional flow area $A(x)$ varies slowly, the nozzle is long and slender, and cross-flow velocities are small, the flow can be modeled as quasi-1D (see, *e.g.*, [8]),

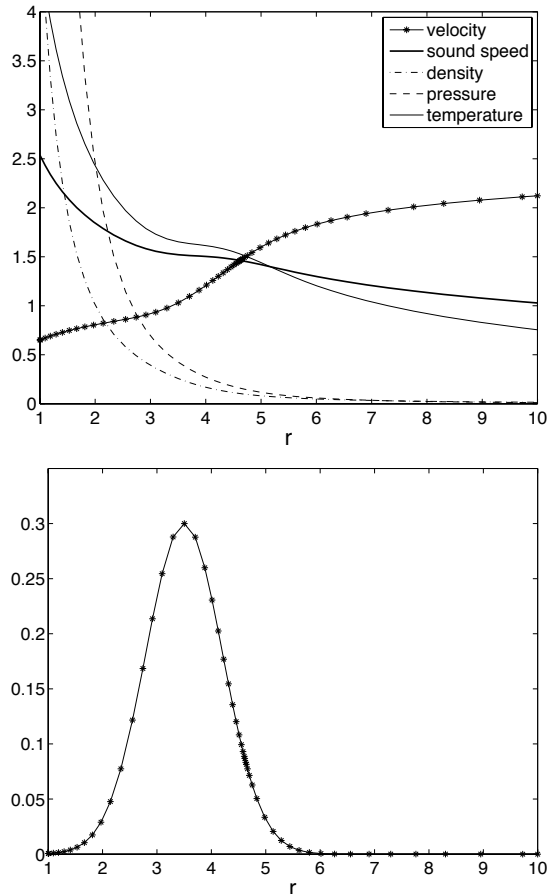


Figure 4: Radial transonic flow solution obtained by the NCP method for a problem with a heating source term. The heating profile (bottom) is $q_{heat}(r) = 0.3 \exp(-(r - 3.5)^2)$.

leading to the following equation system:

$$\frac{\partial}{\partial t} \begin{bmatrix} \rho A \\ \rho u A \\ \left(\frac{p}{\gamma-1} + \frac{\rho u^2}{2}\right) A \end{bmatrix} + \frac{\partial}{\partial x} \begin{bmatrix} \rho u A \\ \rho u^2 A + p A \\ \left(\frac{\gamma p}{\gamma-1} + \frac{\rho u^2}{2}\right) u A \end{bmatrix} = \begin{bmatrix} 0 \\ p \frac{dA}{dx} \\ 0 \end{bmatrix}. \quad (12)$$

The dynamical system associated with the stationary

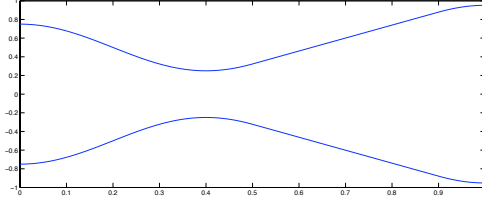


Figure 5: Converging-diverging nozzle. Subsonic flow enters from the left, and is accelerated to supersonic speeds in the nozzle.

part of Eq. (13) can be derived as above, leading to

$$\begin{aligned} \frac{dx}{ds} &= u^2 - c^2, \\ \frac{dF}{ds} &= 0, \end{aligned} \quad (13)$$

$$\begin{aligned} \frac{du}{ds} &= \frac{\gamma u T}{A} \frac{dA}{dx}, \\ \frac{dT}{ds} &= -\frac{(\gamma-1)u^2 T}{A} \frac{dA}{dx}. \end{aligned}$$

The critical points of dynamical system (13) satisfy the two conditions

$$\begin{aligned} u_{crit} &= \sqrt{\gamma T_{crit}} = c_{crit}, \\ \frac{dA}{dx}(x_{crit}) &= 0. \end{aligned} \quad (14)$$

This dynamical system has, thus, a sonic critical point, which can only occur at the throat of the nozzle, where $dA(x)/dx = 0$. The type of the critical point can be determined by investigating the eigenvalues of the Jacobian matrix, which are given by

$$\begin{aligned} \lambda_1 &= 0, \\ \lambda_2 &= 0, \\ \lambda_3 &= \sqrt{\frac{\gamma+1}{A} \frac{d^2A}{dx^2}} u^2, \\ \lambda_4 &= -\sqrt{\frac{\gamma+1}{A} \frac{d^2A}{dx^2}} u^2. \end{aligned} \quad (15)$$

This shows that the sonic critical point is a saddle point at the throat of the nozzle (where $d^2A(x)/dx^2 \geq 0$).

The NCP method described in the previous section can be applied to transonic nozzle flow as follows. In the nozzle case, the location of the critical point is known (it is located at the nozzle throat), so integration can always proceed from the nozzle throat. The

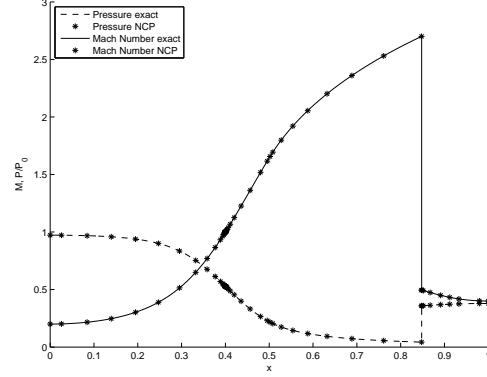


Figure 6: Transonic nozzle flow with shock. The subsonic inflow boundary conditions at the left boundary are given by $p = 0.972497$ and $\rho = p^{1/\gamma}$, and the subsonic outflow boundary condition at the right boundary is given by $p = 0.37917$. The numerical solution obtained by the NCP method is compared with the exact solution.

two-parameter family of critical points can now, for example, be parametrized by $\mathbf{C} = [F_{crit} \ T_{crit}]^T$, and the NCP method can be applied as above for determining the critical point values that match the inflow boundary condition. Note that the NCP method reduces to a regular Newton nonlinear shooting method for the nozzle case. Fig. 6 shows an example of a transonic flow profile that was calculated in this way for the nozzle of Fig. 5. In this example, however, we impose an additional subsonic boundary condition at the outflow, resulting in a shock in the diverging part of the nozzle. This subsonic inflow-subsonic outflow boundary value problem (BVP) can be solved using direct solution of the stationary equations, by extending the NCP method as follows.

Given a certain shock location x_s , the flow state at the left of the shock is determined by the transonic solution calculated as described above, while the state at the right of the shock can be derived from the Rankine-Hugoniot relations at the stationary shock,

$$\begin{aligned} \frac{p_r}{p_l} &= 1 + \frac{2\gamma}{(\gamma+1)} (M_l^2 - 1), \\ \frac{\rho_r}{\rho_l} &= \frac{(\gamma+1)M_l^2}{(\gamma-1)M_l^2 + 2}, \\ \frac{u_l}{u_r} &= \frac{\rho_r}{\rho_l}. \end{aligned} \quad (16)$$

The solution at the outflow boundary x_b for shock location x_s can then be calculated by straightforward ODE integration from the shock to the right boundary. This means that, for example, the pressure at the outflow

boundary can be related to the shock position by some nonlinear mapping f :

$$p(x_b) = f(x_s). \quad (17)$$

If the BVP specifies the pressure at the outflow boundary, $p^*(x_b)$, then nonlinear equation

$$p^*(x_b) = f(x_s). \quad (18)$$

can be solved for the unknown shock location x_s by means of the NCP procedure described above. Fig. 6 shows the result of this procedure applied to a transonic nozzle problem with a shock. Again, only a handful Newton iterations are required to achieve convergence. Note that for this flow we opted to obtain the solution in two separate stages. In the first stage, the transonic profile through the critical point was calculated that matches the left inflow boundary conditions. This calculation can be carried out without consideration of the shock. In the second stage, the shock location and the flow profile downstream from the shock are calculated, using the solution of the first stage of the calculation.

5 CONCLUSION

We have presented the Newton Critical Point method for fast and accurate calculation of 1D transonic solutions of the steady compressible Euler equations. The method is based on adaptive numerical integration outward from the critical point, and uses a dynamical systems formulation of the stationary equations to determine the direction of integration in the neighbourhood of the critical point. The values at the critical point that match the inflow boundary conditions are obtained using a Newton method. It has been shown that the method converges fast and that the solution is accurate. Extension of the method to flows with shocks has been described, and the method has been illustrated for radial outflow problems and quasi-1D nozzle flows.

The NCP method is much more efficient than traditional methods that are based on time-marching of the time-dependent equations, and is more accurate. Explicit relaxation methods for calculating stationary transonic flow profiles require up to several thousands of full integration sweeps over the problem domain. Relaxation methods based on implicit discretization of the time-dependent equations may also require only a limited number of Newton-like iterations, but each step requires the inversion of a large Jacobian matrix that contains all the discrete degree of freedoms, while in our approach the Newton system to be solved is a small 2×2 system. In addition, the NCP method is

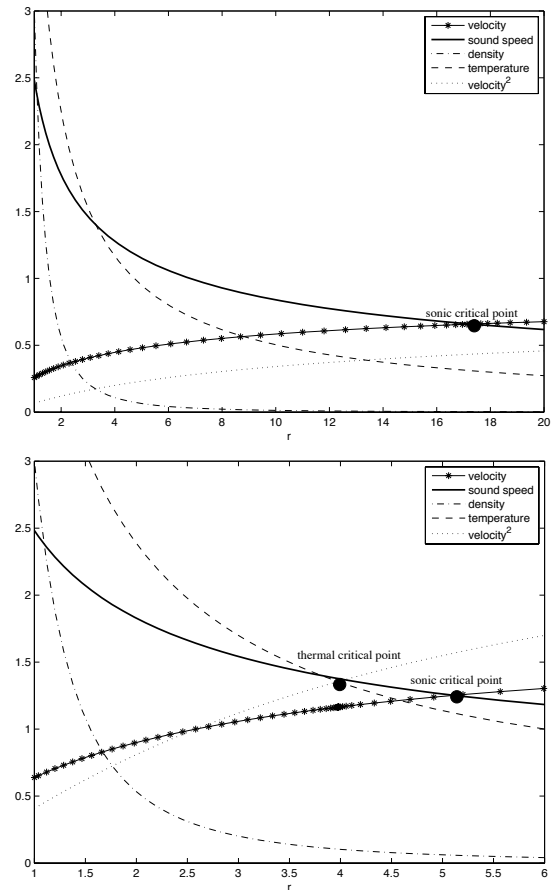


Figure 7: BVP flow trajectories without (top) and with (bottom) heat conduction. Both flow solutions have $\rho = 3$ and $T = 4.4$ at the inflow boundary. In addition, $dT/dr = -4$ is imposed at the inflow boundary for the bottom solution.

more accurate than time-stepping methods, due to the use of adaptive integration based on rigorous error estimation. It is thus clear that the NCP method offers an efficient and accurate alternative to these existing methods for 1D problems.

As described in [9], the NCP method can be extended to transonic flow profiles with heat conduction. It turns out that, in this case, a new critical point appears, at which $u = c/\sqrt{\gamma}$. This so-called thermal critical point takes over the saddle-point role of the sonic critical point. Fig. 7 shows a radial transonic flow profile obtained by the NCP method for a problem with heat conduction.

The NCP method as described in this paper deals with transonic flows in one dimension. The ideas behind the algorithm, however, are quite general. Application of

these ideas to problems in multiple spatial dimensions is a promising topic of further research.

REFERENCES

- [1] Feng Tian, Owen B. Toon, Alexander A. Pavlov, and H. De Sterck. Transonic Hydrodynamic Escape of Hydrogen from Extrasolar Planetary Atmospheres. *Astrophysical Journal*, 621:1049-1060, 2005.
- [2] Feng Tian, Owen B. Toon, Alexander A. Pavlov, and H. De Sterck. A Hydrogen-Rich Early Earth Atmosphere. *Science*, 308:1014-1017, 2005.
- [3] R.J. LeVeque. Finite volume methods for hyperbolic problems. Cambridge University Press, Cambridge, 2002.
- [4] B. van Leer, W.T. Lee and P.L. Roe. Characteristic time-stepping or local preconditioning of the Euler equations. *AIAA Paper* 91-1552, 1991.
- [5] D.L. Darmofal and K. Siu. A Robust Multigrid Algorithm for the Euler Equations with Local Preconditioning and Semi-coarsening. *Journal of Computational Physics*, 151:728-756, 1999.
- [6] Bernd Krauskopf, Hinke M. Osinga, Eusebius J. Doedel, Michael E. Henderson, John M. Guckenheimer, Alexander Vladimírsky, Michael Dellnitz and Oliver Junge. A survey of methods for computing (un)stable manifolds of vector fields. *Int. J. Bifurcation & Chaos*, 15:763-791, 2005.
- [7] Lars Elden, Linde Wittmeyer-Koch, and Hans Bruun Nielsen. Introduction To Numerical Computation. Studentlitteratur AB, Lund, 2004.
- [8] G. I. Benison and E. L. Rubin. A time-dependent analysis for quasi-one-dimensional, viscous, heat conducting, compressible Laval nozzle flows. *Journal of Engineering Mathematics*, 5:39-49, 1970.
- [9] H. De Sterck. Critical point analysis of transonic flow solutions with heat conduction. *Submitted to SIAM J. Appl. Dyn. Syst*, 2006.